RESEARCH FRONT

CSIRO PUBLISHING

Aust. J. Chem. **2013**, *66*, 864–873
http://dx.doi.org/10.1071/CH13219

Full Paper

Synthesis, Structural Characterisation, and Preliminary Evaluation of Non-Indolin-2-one-based Angiogenesis Inhibitors Related to Sunitinib (Sutent®)

Pichit Sudta,[A,F] *Nicholas Kirk,*[B,F] *Anna Bezos,*[C] *Anthony Gurlica,*[B] *Rhys Mitchell,*[B] *Thomas Weber,*[B] *Anthony C. Willis,*[D] *Samran Prabpai,*[E] *Palangpon Kongsaeree,*[E] *Christopher R. Parish,*[C] *Sunit Suksamrarn,*[A] *and Michael J. Kelso*[B,G]

[A]Department of Chemistry, Faculty of Science, Srinakharinwirot University, Bangkok 10110, Thailand.
[B]School of Chemistry, Faculty of Science, University of Wollongong, Wollongong, NSW 2522, Australia.
[C]Cancer and Vascular Biology Group, Department of Immunology, John Curtin School of Medical Research, Australian National University, Canberra, ACT 2600, Australia.
[D]Single-crystal X-ray Diffraction Unit, Research School of Chemistry, Australian National University, Canberra, ACT 2600, Australia.
[E]Centre for Excellence in Protein Structure and Function, Faculty of Science, Mahidol University, Bangkok 10400, Thailand.
[F]These authors contributed equally to this work.
[G]Corresponding author. Email: mkelso@uow.edu.au

The indolin-2-one fused-ring system and the 2,4-dimethylpyrrole unit represent key structural motifs in the anticancer drug sunitinib (Sutent®) and predecessor angiogenesis inhibitors that have undergone anticancer clinical trials (e.g. semaxanib, SU5416). In pursuit of novel anti-angiogenic scaffolds, we were interested in identifying whether the indolin-2-one group in these structures could be modified without losing activity. This paper describes novel condensation chemistry used to prepare a test series of (*E*)- and (*Z*)-alkenes related to SU5416 that retain the 2,4-dimethylpyrrole unit while incorporating ring-opened indolin-2-ones. Unique structural characteristics were identified in the compounds, such as intramolecular hydrogen bonds in the (*Z*)-alkenes, and several examples were shown to possess significant anti-angiogenic activity in a rat aorta in vitro model of angiogenesis. The work demonstrates that the indolin-2-one moiety is not an absolute requirement for angiogenesis inhibition in the sunitinib/SU5416 class.

Manuscript received: 29 April 2013.
Manuscript accepted: 24 May 2013.
Published online: 20 June 2013.

Introduction

Angiogenesis, the growth of new blood vessels from pre-existing vascular networks, occurs only under certain conditions in adults, such as during wound healing, pregnancy, and menstruation, but can be much more prevalent in pathological conditions, especially cancer.[1,2] Solid tumours that grow beyond ~1–2 mm require angiogenesis to avoid becoming hypoxic from the effects of growth factor mutation-induced aberrant blood vessel formation and increased energy consumption.[3] In the absence of angiogenesis, solid tumours enter latent phases and rely on anaerobic metabolism for energy, limiting their growth.[2,3] Angiogenesis is also a major contributor to metastasis as the newly formed vessels provide a route for tumour cells to enter the circulation.[3] Accordingly, inhibitors of angiogenesis have been intensely studied as anticancer agents and several have been approved for clinical use.[4]

The first FDA-approved angiogenesis inhibitor was the vascular endothelial growth factor (VEGF)-targeting monoclonal antibody (Mab) bevacizumab (Avastin®; Genentech Inc., San Francisco, 2003), which continues to be used today in combination therapies against metastatic colorectal cancer,[5] non-small-cell lung cancer,[6] and metastatic breast cancer.[7] Newer VEGF-targeting agents are in various stages of clinical development, including, for example, VEGF-Trap$_{R1R2}$ (Aflibercept, Regeneron Inc.), a chimeric soluble VEGF receptor that binds to and neutralises VEGF.[8] In addition to these biologics, small-molecule-receptor tyrosine kinase inhibitors (RTKIs) targeting VEGF receptors (VEGFR1−VEGFR3) and

other kinase signalling pathways have been extensively investigated as anti-angiogenics and several have progressed to the market. These include sunitinib **1** (Sutent®, Pfizer),[9] pazopanib (Votrient®, GSK),[10] sorafenib (Nexavar®, Bayer),[11] and vandetanib (Caprelsa®, AstraZeneca).[12]

Sunitinib **1** (Fig. 1) is approved for the treatment of highly vascularised renal cell carcinomas,[13] gastrointestinal stromal tumours,[14] and pancreatic neuroendocrine tumours.[15] Its mechanism of action involves inhibition of at least eight different receptor tyrosine kinases, including VEGF1–VEGF3, platelet-derived growth factor receptors (PDGFRα and PDGFRβ), stem-cell factor receptor (Kit), Fms-like tyrosine kinase 3 (FLT-3), and colony-stimulating factor-1 receptor (CSF-1R).[16] During development, the indolin-2-one (oxindole) and 2,4-dimethylpyrrole portions of Sunitinib **1** were identified as key pharmacophores and retained throughout med-chem optimisation efforts. Several other closely related compounds that contain these groups were also (and continue to be) evaluated in clinical trials.[17] For example, the structurally simpler sunitinib predecessor semaxanib (SU5416) **2** (Fig. 1) underwent a Phase III clinical trial for advanced colorectal cancer.

In pursuit of novel and patentable anti-angiogenic scaffolds, we hypothesised that in spite of its perceived importance, the indolin-2-one moiety may not be essential for anti-angiogenic activity in the sunitinib/SU5416 class. The hypothesis has been explored in the current work using a test series of SU5416-like alkenes that attach the 2,4-dimethylpyrrole unit to ring-opened indolin-2-ones (i.e. compounds (*Z*)-**3a**, (*E*)-**3b**–(*Z*)-**10a**, (*E*)-**10b**, Fig. 1). This paper details the synthesis of the series using novel condensation chemistry, describes some of the unique structural characteristics of the alkenes, as identified by NMR spectroscopy and X-ray crystallography, and reports that several members show significant anti-angiogenic activity in a rat aorta in vitro model of angiogenesis.

Chemistry

Initial synthetic efforts aimed to identify a general condensation reaction that could provide access to the target alkenes. In the reported syntheses of sunitinib **1**, SU5416 **2**, and related indolin-2-ones, the base indolin-2-ones and requisite *N*-unsubstituted pyrrole-2-carboxaldehydes were condensed by refluxing the two components in ethanol with piperidine.[18] Attempts to adapt this procedure to the condensation of the model substrate ethyl-2-(2-nitrophenyl)acetate **13** and 3,5-dimethylpyrrole-2-carboxaldehyde **11** failed to yield any of the desired alkenes (*Z*)-**3a** or (*E*)-**3b**. Other Knoevenagel or Perkin-type condensations attempted with **13** and **11** using various bases and solvents and under a variety of conditions were similarly unsuccessful. At this point, it was reasoned that the aldehyde in **11** was unreactive owing to a combination of steric hindrance from the neighbouring pyrrole 3-Me group and because electron donation from the pyrrole nitrogen into the aldehyde was reducing its electrophilic character. It was postulated that a small electron-withdrawing group attached to the pyrrole nitrogen should increase the aldehyde's reactivity without increasing steric hindrance. Attaching electron-withdrawing groups to pyrrole nitrogens has previously been shown to activate aldehydes at the 2-position.[19,20] Accordingly, *N*-methylcarbamoyl pyrrole-2-carboxaldehyde **12** was prepared in 86 % yield by acylating the potassium salt of **11** (formed by *N*-deprotonation of **11** with KH in THF at 0°C) with methyl chloroformate (Scheme 1).

Stirring ethyl-2-(2-nitrophenyl)acetate **13** with **12** in refluxing THF in the presence of K_2CO_3 and 18-crown-6 (Method a,

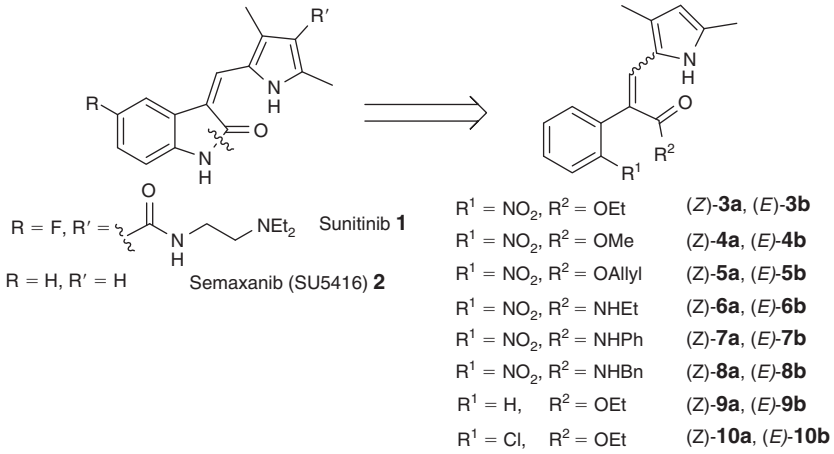

Fig. 1. Structures of sunitinib **1**, semaxanib (SU5416) **2**, and alkenes (*Z*)-**3a**, (*E*)-**3b**–(*Z*)-**10a**, (*E*)-**10b**.

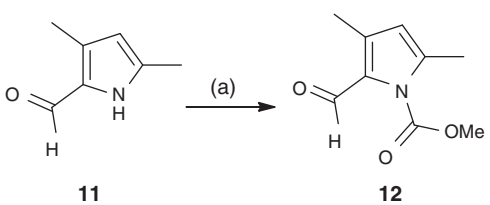

Scheme 1. Synthesis of *N*-methylcarbamoyl pyrrole aldehyde **12**. Reagents and conditions: (a) (i) KH, THF, 0°C; (ii) CH_3OCOCl, 2 h (86 %).

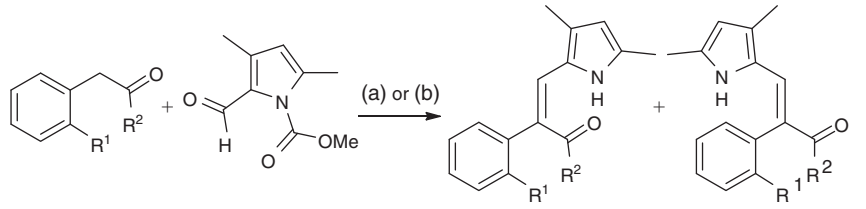

Phenylacetic Ester[B]/Amide[C]	R^1	R^2	Reaction conditions	Product, yield [%]	Product, yield [%]
13	NO_2	OEt	a	(*Z*)-**3a**, 42	(*E*)-**3b**, 35
14	NO_2	OMe	a	(*Z*)-**4a**, 36	(*E*)-**4b**, 40
15	NO_2	OAll	a	(*Z*)-**5a**, 41	(*E*)-**5b**, 33
16	NO_2	NHEt	a	(*Z*)-**6a**, 21	(*E*)-**6b**, 0
17	NO_2	NHPh	a	(*Z*)-**7a**, 22	(*E*)-**7b**, <5[A]
18	NO_2	NHBn	a	(*Z*)-**8a**, 16	(*E*)-**8b**, <5[A]
19	H	OEt	b	(*Z*)-**9a**, 0	(*E*)-**9b**, 32
20	Cl	OEt	b	(*Z*)-**10a**, 5	(*E*)-**10b**, 41

[A]Compounds could not be isolated in pure form.
[B]Esters **13**–**15**, **19**, **20** were synthesised by refluxing the phenylacetic acids in the requisite alcohol (as solvent) with H_2SO_4 (cat.).
[C]Amides **16**–**18** were obtained by stirring 2-nitrophenylacetic acid with the requisite amines under standard solution-phase peptide coupling conditions (i.e. HBTU/DIPEA in CH_2Cl_2).

Fig. 2. Synthesis of alkenes (*Z*)-**3a**, (*E*)-**3b**–(*Z*)-**10a**, (*E*)-**10b**. Reagents and conditions: (a) K_2CO_3, 18-crown-6, THF, reflux, 16 h; (b) LDA, THF, −78°C, 30 min.

Fig. 2) was found to directly afford the pyrrole *N*-deprotected Knoevenagel condensation products (*Z*)-**3a** (42 %) and (*E*)-**3b** (35 %). Similar yields of the desired *N*-deprotected (*Z*)- and (*E*)-alkenes were obtained directly from reactions of **12** with methyl-2-(2-nitrophenyl)acetate **14** and allyl-2-(2-nitrophenyl) acetate **15** (i.e. (*Z*)-**4a**, (*E*)-**4b** and (*Z*)-**5a**, (*E*)-**5b** respectively). The condensation reactions did not proceed when the *N*-methyl carbamoyl group of **12** was replaced with either *N*-ethyl or *N*-^{t}butyl carbamates, possibly owing to increased steric hindrance around the aldehyde.

Use of *N*-alky- or *N*-aryl-2-(2-nitrophenyl)acetamides in place of 2-(2-nitrophenyl)acetic esters led to reduced yields of the *Z*-isomers and none or very low yields of the *E*-isomers. Nevertheless, several amides were able to be isolated in sufficient quantity and purity (>95 % by ^{1}H NMR) for characterisation and angiogenesis inhibition testing. Use of *N*-ethyl-2-(2-nitrophenyl)acetamide **16** in the reaction afforded a 21 % yield of (*Z*)-**6a** without formation of any (*E*)-**6b**. *N*-Phenyl-2-(2-nitrophenyl)acetamide **17** and *N*-benzyl-2-(2-nitrophenyl) acetamide **18** yielded 22 and 16 % yields respectively of alkenes (*Z*)-**7a** and (*Z*)-**8a**, with less than 5 % of the *trans* isomers (*E*)-**7b** and (*E*)-**8b** being isolated. All alkenes except (*E*)-**7b** and (*E*)-**8b** were tested for angiogenesis inhibition.

In our structure–activity study, it was of interest to establish the importance of the 2-nitro group for angiogenesis inhibition. Alkenes (*Z*)-**9a**, (*E*)-**9b**, (*Z*)-**10a**, and (*E*)-**10b** were targeted for this purpose. However, attempts to perform the condensation (Fig. 2, Method a) with **12** and either ethyl-2-phenylacetate **19** or ethyl-2-(2-chlorophenyl)acetate **20** were unsuccessful, thus highlighting the requirement for the *ortho*-nitro group in this reaction. Switching to the stronger base lithium-*N*,*N*-diisopropylamide (LDA) and carrying the reaction out with ethyl-2-phenylacetate **19** in THF at −78°C (Fig. 2, Method b) afforded a 32 % yield of the *trans* alkene (*E*)-**9b** whereas none of the *cis* alkene (*Z*)-**9a** was formed. Applying the same procedure with 2-(2-chlorophenyl)acetate **20** yielded 41 % of (*E*)-**10b** and 5 % of the *cis* isomer (*Z*)-**10a**.

Cis-stereochemistry was confirmed in alkenes (*Z*)-**3a**–(*Z*)-**10a** using 2-dimensional nuclear overhauser effect spectroscopy (2D-NOESY) spectra, which in all cases showed NOE crosspeaks between the vinylic proton and the *ortho* proton on the phenyl ring (Fig. 3a). A second feature common to all *cis* isomers was a downfield chemical shift of the pyrrole NH signals (11.80–12.91 ppm) in their ^{1}H NMR spectra relative to the corresponding *trans* isomers (6.47–6.87 ppm, Fig. 3b). These strongly deshielded signals suggested the presence of intramolecular hydrogen bonds in the *cis* alkenes between the pyrrole NH and carbonyl oxygen atoms.[21] Furthermore, the *cis* isomers were all observed to be significantly less polar than their corresponding *trans* isomers (by TLC), which, in addition to simplifying purification by silica gel column chromatography, supported the presence of the hydrogen bonds. The presence of an intramolecular hydrogen bond in allyl ester (*Z*)-**5a** was eventually confirmed (in the solid state) by X-ray crystallography (Fig. 4a). It is noteworthy that analogous hydrogen bonds are found in SU5416 **2** and related indolin-2-one-based angiogenesis inhibitors that contain (*Z*)-alkenes.[22]

The ^{1}H NMR spectrum of (*E*)-**3b** displayed an unusual pair of doublet-of-quartet signals at 4.10 and 4.23 ppm (total integration 2H), suggesting the presence of diastereotopic ethyl ester CH_2 protons (Supplementary Material, Fig. S1b). In contrast, the CH_2 group of (*Z*)-**3a** displayed the expected first-order quartet at 4.12 ppm. (Supplementary Material, Fig. S1 a). Complex methylene signals were similarly observed for the

(a)

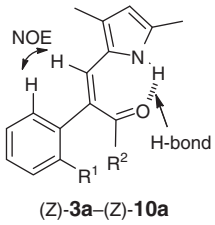

(Z)-**3a**–(Z)-**10a**

(b)

cis-alkenes		*trans*-alkenes	
Compound	Pyrrole NH chemical shift [ppm]	Compound	Pyrrole NH chemical shift [ppm]
(*Z*)-**3a**	11.89	(*E*)-**3b**	6.80
(*Z*)-**3a**	11.82	(*E*)-**4b**	6.74
(*Z*)-**5a**	12.91	(*E*)-**5b**	6.75
(*Z*)-**6a**	12.21	(*E*)-**6b**	N/A
(*Z*)-**7a**	12.00	(*E*)-**7b**	6.47
(*Z*)-**8a**	12.21	(*E*)-**8b**	N/A
(*Z*)-**9a**	N/A	(*E*)-**9b**	6.84
(*Z*)-**10a**	11.80	(*E*)-**10b**	6.75

N/A: not available

Fig. 3. (a) *cis*-Stereochemistry was confirmed in (*Z*)-**3a**–(*Z*)-**10a** by the presence of a nuclear overhauser effect (NOE) between the vinylic proton and *ortho* proton on their respective phenyl rings. (b) Comparison of the pyrrole NH chemical shift values in the ^{1}H NMR spectra of *cis*-alkenes (*Z*)-**3a**–(*Z*)-**10a** and *trans*-alkenes (*E*)-**3b**–(*E*)-**10b**. The downfield-shifted signals in the *cis* series are indicative of intramolecular hydrogen bonds between the pyrrole NH and carbonyl oxygen atoms.

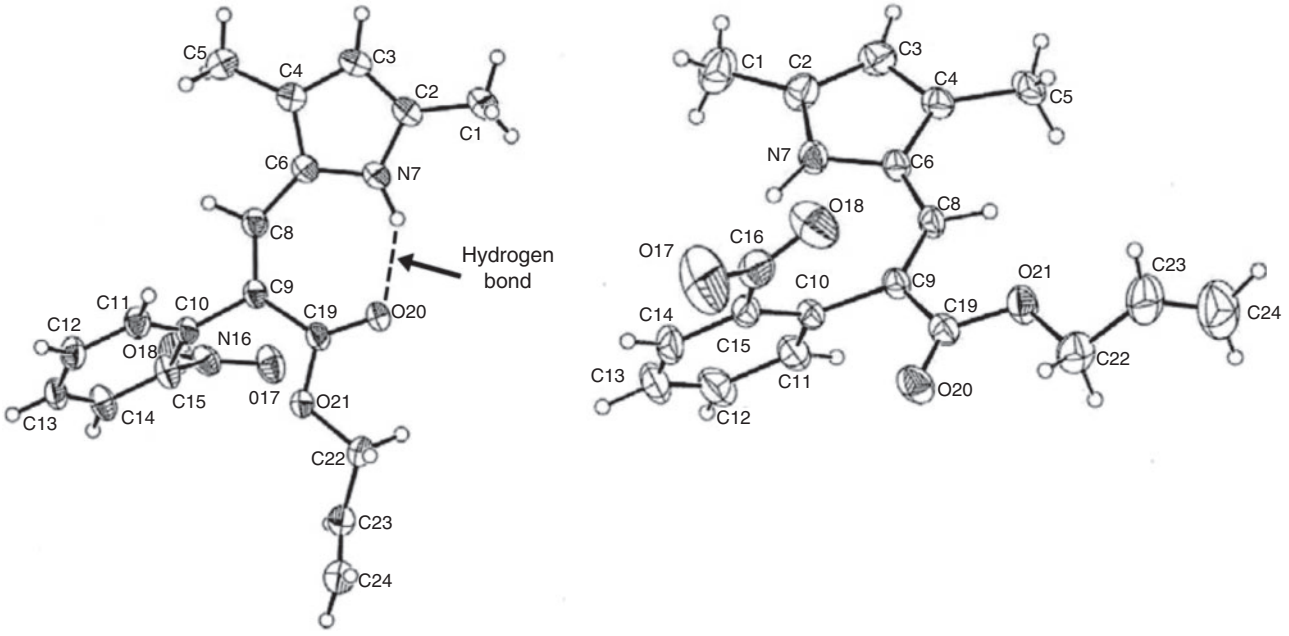

Fig. 4. *ORTEP* plots of allyl esters (a) (*Z*)-**5a**; and (b) (*E*)-**5b**. An intramolecular hydrogen bond was observed in (*Z*)-**5a** between the pyrrole N–H and carbonyl oxygen atoms (N7 to O20 distance = 2.7 Å).

allyl ester methylene CH_2 of (*E*)-**5b** (2 × doublet-of-doublets at 4.59 and 4.64 ppm) and the ethyl ester CH_2 group of (*E*)-**10b** (2 × quartets at 4.18 and 4.25 ppm). Such observations are consistent with the disubstituted phenyl rings of these compounds being unable to freely rotate about the *ipso* Ar–C bond owing to a steric clash between the bulky *ortho* phenyl-ring substituents (i.e. *ortho*-NO_2 in (*E*)-**3b** and (*E*)-**5b**, and *ortho*-Cl in (*E*)-**10b**) and the pyrrole ring located on the same side of the alkene double bond (Supplementary Material, Fig. S1c). The restricted rotation and resulting axial double-bond chirality in these 'overcrowded' alkenes explains the presence of diastereotopic CH_2 signals in the ^{1}H NMR spectra. That the CH_2 group of (*E*)-**9b** (which contains no aryl *ortho* substituent) produced a simple quartet at 4.22 ppm supports this explanation, as does the appearance of the CH_2 groups of *cis*-alkenes (*Z*)-**5a**, (*Z*)-**6a**, and (*Z*)-**10a** as first-order quartets (integration 2H), and the benzyl CH_2 group of (*Z*)-**8a** as a simple doublet (integration 2H).

Single-crystal X-ray structures were obtained for the pair of allyl esters (*Z*)-**5a** and (*E*)-**5b** (Fig. 4). The solid-state structure of (*Z*)-**5a** provided clear evidence for an intramolecular hydrogen bond stabilising a pseudo-7-membered ring within its structure. The interatomic distance between the pyrrole nitrogen and the carbonyl oxygens atom in the crystal structure was very short (2.7 Å), suggesting that the hydrogen bond in (*Z*)-**5a** is relatively strong.[21] The X-ray structure of (*E*)-**5b** showed no intramolecular hydrogen bonds.

Angiogenesis Inhibition

The alkenes were tested for anti-angiogenic effects using our previously reported rat aorta in vitro model of angiogenesis

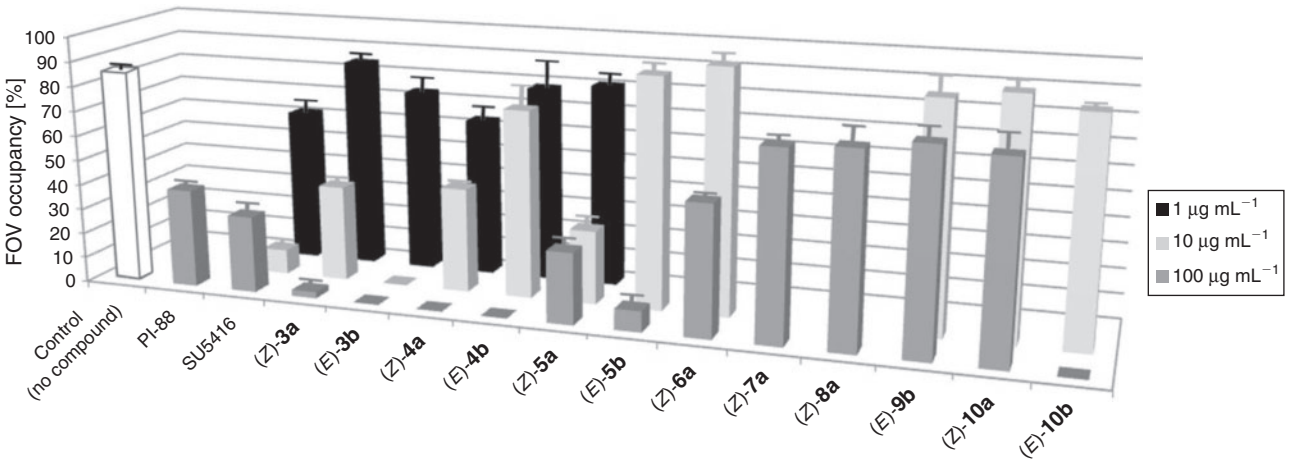

Fig. 5. Inhibition of angiogenesis by alkenes (*Z*)-**3a**, (*E*)-**3b**–(*Z*)-**10a**, (*E*)-**10b** relative to negative control (no compound) and positive controls PI-88[24] (100 μg mL^{-1}) and SU5416 **2**. Female Fischer 344 rat thoracic aortic sections were cultured in a gel fibrin matrix in 48-well plates in the presence or absence of compounds. Cultures were fed on Day 4 and vessel outgrowths measured on Day 5.[23] Wells were visualised under 40× magnification and the percentage of the field of view (FOV) occupied by vessel outgrowths reported as FOV occupancy. Negative control (no compound, unshaded bar) showed 85.7 % FOV occupancy. Compounds showing little or no activity at higher concentrations were not tested at lower concentration. Data represent the mean FOV occupancy (%) generated from at least six replicate cultures of each test compound at each concentration tested (see Supplementary Material Table S1 for statistics).

(Fig. 5).[23] In this assay, thoracic aortic sections are excised from female Fischer 344 rats and suspended in a fibrin gel matrix in 48-well plates. A minimum of six replicate cultures for each compound treatment (at each concentration) are prepared. The cultures are fed on Day 4 and vessel outgrowths from the rings measured on Day 5. Angiogenesis is visualised under a microscope (40× magnification) and quantified manually as the percentage of the field of view (FOV) around the vessel fragment occupied by new vessel outgrowths (i.e. FOV %). Under these conditions, absence of test compound produces 85.7 % FOV occupancy (Fig. 5; control: no compound).

Two positive controls PI-88 and SU5416 **2** were included in the assays. PI-88 is a highly sulfated oligosaccharide-based angiogenesis inhibitor[24] currently undergoing Phase III clinical trials as a single treatment following cancer surgery in subjects with hepatitis virus-related hepatocellular carcinoma.[25] At 100 μg mL^{-1}, PI-88 reduced FOV occupancy to 39.2 %. SU5416 **2** produced an unusual response where greater inhibition of angiogenesis was observed at 10 μg mL^{-1} (FOV occupancy 9.7 %) than at 100 μg mL^{-1} (FOV occupancy 30.6 %), whereas 61.4 % FOV occupancy was observed at 1 μg mL^{-1}. Small crystals observed in wells containing 100 μg mL^{-1} SU5416 **2** suggested that its low solubility in the medium may have caused the poor dose dependency.

Ethyl and methyl esters (*Z*)-**3a**, (*E*)-**3b**, (*Z*)-**4a**, and (*E*)-**4b** were found to completely inhibit angiogenesis at 100 μg mL^{-1}. At 10 μg mL^{-1}, (*E*)-**3b** continued to show complete inhibition whereas the other three esters all showed significantly diminished effects at this concentration. At 1 μg mL^{-1}, the four esters showed either minimal effects (<20 % difference relative to negative control) or no activity. Surprisingly, the *cis*-allyl ester (*Z*)-**5a** showed the same level of inhibition at both 100 and 10 μg mL^{-1} (FOV occupancy 28.3 and 29.3 % respectively) but no activity at 1 μg mL^{-1}. For the *trans*-allyl ester (*E*)-**5b**, strong activity was observed at 100 μg mL^{-1} (FOV occupancy 8.3 %) but this activity was completely lost at 10 μg mL^{-1}. We conclude from the data that (*E*)-**3b** is the most active of the 2-nitrophenylacetic ester series.

The c*is*-ethylamide (*Z*)-**6a** showed reduced effects (FOV occupancy 51.7 % at 100 μg mL^{-1}, inactive at 10 μg mL^{-1}) relative to (*Z*)-**3a**, indicating that directly substituting the ester group for an amide is detrimental for activity. Observing that amides (*Z*)-**7a** and (*Z*)-**8a** were inactive at 100 μg mL^{-1} supported this conclusion. Removal of the NO_2 group from the phenyl ring was found to completely abolish activity (i.e. (*E*)-**9b** v. (*E*)-**3b**). Interestingly, replacing the NO_2 group with Cl had no effect on activity at 100 μg mL^{-1}, with both (*E*)-**10b** and (*E*)-**3b** completely inhibiting angiogenesis, but at 10 μg mL^{-1} (*E*)-**10b** showed no activity.

Visual inspection of the assay wells on Day 5 revealed that outgrowths sprouting from rings cultured in the presence of SU5416 **2** (100 μg mL^{-1}) differed markedly in morphology from those sprouting from control rings (no compound) or from rings cultured in the presence of PI-88 (100 μg mL^{-1}) or alkenes (e.g. (*Z*)-**3a**, 100 μg mL^{-1}) (Fig. 6). Whereas the outgrowths from the control rings and rings grown in the presence of PI-88 or alkenes showed normal morphology, outgrowths from the SU5416 **2**-treated rings consisted of fine hair-like structures that lacked a visible lumen. At lower concentrations of SU5416 **2** (10 μg mL^{-1}), the outgrowths showed normal morphology.

Concluding Remarks

In summary, a novel series of alkenes (*Z*)-**3a**, (*E*)-**3b**–(*Z*)-**10a**, (*E*)-**10b** was synthesised to test the hypothesis that anti-angiogenic activity can be retained in structures related to semaxanib (SU5416) **2**, a structurally simpler predecessor of the FDA-approved drug sunitinib, when the indolin-2-one moiety is modified through ring-opening. The 2,4-dimethylpyrrole portion of SU5416 **2** was retained in the test compounds to strengthen conclusions regarding the importance of the indolin-2-one group. In vitro angiogenesis inhibition assays revealed that several of the alkene esters, including both (*Z*)- and (*E*)-isomers, showed significant anti-angiogenic effects. Compound (*E*)-**3b** emerged as the most potent, showing complete inhibition of angiogenesis at 10 μg mL^{-1}. The work provides

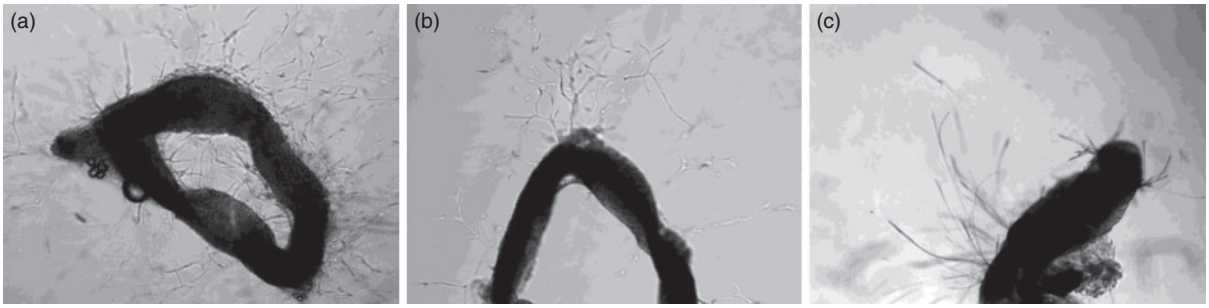

Fig. 6. Morphology of vessel outgrowths from rat aortic rings cultured in the presence of: (a) control (no compound); (b) PI-88 (100 μg mL^{-1}); and (c) SU5416 **2** (100 μg mL^{-1}). The outgrowths from control rings and rings grown in the presence of PI-88 (and (*Z*)-**3a**; image not shown) appeared normal whereas rings cultured in the presence SU5416 **2** produced fine hair-like outgrowths with no lumen.

evidence that the indolin-2-one moiety is not essential for anti-angiogenic activity in the sunitinib/SU5416-type class.

The novel condensation chemistry developed to access the target series has scope for wider exploration. For example, whereas the *ortho*-NO_2 group was found to be necessary for successful reactions with phenylacetic esters and amides, it would be of interest to explore whether this group can be moved to the *meta* or *para* positions on the phenyl ring and whether it can be replaced altogether with other electron-withdrawing groups. Additionally, it is likely that **12** could be useful as a 3,5-dimethylpyrrole-2-carboxaldehyde surrogate in condensation reactions with carbanions derived from substrates other than phenylacetic esters and amides. It is also tempting to speculate that pyrrole *N*-methyl carbamoylation might be a more generally useful tactic in condensation reactions with other pyrrole-2-carboxaldehydes where either enhanced aldehyde reactivity or pyrrole *N*-protection is required.

Experimental

Chemistry

3,5-Dimethylpyrrole-2-carboxaldehyde **11** was purchased from Sigma–Aldrich. Semaxanib (SU5416) **2** was synthesised in-house using a novel (unpublished) procedure. The spectroscopic data for the synthesised Semaxanib was identical in all respects to that reported in the literature.[22] Anhydrous tetrahydrofuran (THF) was freshly distilled from sodium benzophenone ketyl. Anhydrous CH_2Cl_2 was freshly distilled from CaH_2. All other solvents were of analytical reagent (AR) grade and used without further purification. The term petroleum spirit refers to that within the boiling range 40–60°C. Column chromatography was performed using silica gel 60 (230–400 mesh, Merck). Reaction monitoring by TLC was carried out using Merck silica gel 60 F254 (0.2 mm) plates. Compounds were visualised by examination under UV light or by staining with cerium ammonium molybdate. ^{1}H and ^{13}C NMR spectra were recorded on a Varian Inova-500 MHz spectrometer. Chemical shifts (δ) are expressed in ppm relative to tetramethylsilane (0 ppm). Signal splitting patterns are described as singlet (s), broad singlet (br s), doublet (d), triplet (t), broad triplet (br t), quartet (q), multiplet (m) or a combination of the above. IR spectra were recorded using a Nicolet Avatar 360 Fourier-transform (FT)-IR spectrometer with characteristic absorption bands reported in wavenumbers (cm^{-1}). High-resolution electrospray ionisation mass spectra (HRMS-ESI) were recorded using a factory-modified Waters QToF Ultima Mass Spectrometer (Wythenshawe, UK). Melting points were determined using a Reichert melting point apparatus and are uncorrected.

*Methyl 2-Formyl-3,5-dimethyl-1*H*-pyrrole-1-carboxylate (**12**)*

3,5-Dimethylpyrrole-2-carboxaldehyde **11** (1.47 g, 11.9 mmol) in anhydrous THF (10 mL) was added dropwise over 10 min to a stirring suspension of potassium hydride (0.57 g, 14.3 mmol) in dry THF (50 mL) under N_2 at 0°C. Following complete addition, the mixture was stirred at 0°C for a further 30 min. Methyl chloroformate (2.48 g, 26.2 mmol) diluted in anhydrous THF (10 mL) was then added dropwise to the stirring mixture at 0°C over 10 min. The reaction was allowed to warm slowly to room temperature and stirred for a further 2 h while monitoring by TLC analysis (petroleum spirit/acetone, 80 : 20). After complete consumption of starting material, the reaction was quenched with ice-cold H_2O (30 mL) and stirred for 15 min. The crude mixture was extracted with EtOAc (3 × 25 mL) and the combined organic extracts washed with H_2O (25 mL) and brine (25 mL) before drying over anhydrous $MgSO_4$ and concentrating under vacuum. The crude product was purified by silica gel column chromatography using a gradient from 100 : 0 to 95 : 5 petroleum spirit/acetone to provide **12** (1.83 g, 85 %) as a white crystalline solid. R_f 0.53 (80 : 20 petroleum spirit/acetone), mp 44–45°C. δ_H (500 MHz, $CDCl_3$) 2.34 (s, 3H), 2.42 (s, 3H), 4.00 (s, 3H), 5.93 (s, 1H), 10.03 (s, 1H). δ_C (125 MHz, $CDCl_3$) 12.9, 15.2, 54.3, 115.9, 130.3, 135.8, 138.2, 151.5, 181.2. ν_{max} (neat)/cm^{-1} 1730, 1650, 1496, 1451, 1326, 1153, 765. *m/z* (HRMS-ESI) 182.0817 $[M+H]^+$; $C_9H_{11}NO_3$ requires 182.0812.

*General Method for the Synthesis of 2-Phenylacetic Esters **13**–**15**, **19**, **20***

A solution of the requisite 2-phenylacetic acid (~3 g) in the appropriate alcohol (40 mL) with 5 drops of concentrated sulfuric acid added was stirred at reflux under N_2. On complete disappearance of starting material (TLC; petroleum spirit/acetone, 70 : 30), the reaction mixture was allowed to cool to room temperature before removing the alcohol by evaporation under vacuum. The crude residue was diluted with EtOAc (50 mL), added to a separating funnel and washed with saturated aqueous Na_2CO_3 (30 mL), H_2O (3 × 25 mL), and brine (30 mL). The organic layer was then dried over anhydrous $MgSO_4$ and concentrated under vacuum.

*Ethyl-2-(2-nitrophenyl)acetate (**13**)*

Yield: 97 %, white crystalline solid; mp 61–63°C. δ_H (500 MHz, $CDCl_3$) 1.16 (t, 3H, *J* 7.0), 3.93 (s, 2H), 4.07 (q, 2H, *J* 7.0), 7.28 (d, 1H, *J* 7.5), 7.38 (t, 1H, *J* 8.0), 7.50 (t, 1H, *J* 7.5), 7.99 (d, 1H, *J* 8.0). δ_C (125 MHz, $CDCl_3$) 13.7,

39.4, 60.9, 124.9, 128.2, 129.5, 132.9, 133.2, 148.5, 170.0. *m/z* (HRMS-ESI) 210.075 $[M+H]^+$; $C_{10}H_{12}NO_4$ requires 210.0761.

*Methyl-2-(2-nitrophenyl)acetate (**14**)*

Yield: 97 %, pale yellow oil. δ_H (500 MHz, $CDCl_3$) 3.68 (s, 3H), 4.00 (s, 2H), 7.34 (d, 1H, *J* 8.0), 7.45 (t, 1H, *J* 8.0), 7.57 (t, 1H, *J* 8.0), 8.08 (d, 1H, *J* 8.0). δ_C (125 MHz, $CDCl_3$) 39.8, 52.5, 125.5, 128.9, 133.5, 133.6, 133.8, 148.9, 170.6. *m/z* (HRMS-ESI) 196.0615 $[M+H]^+$; $C_9H_{10}NO_4$ requires 196.0604.

*Allyl-2-(2-nitrophenyl)acetate (**15**)*

Yield: 88 %, pale yellow oil. δ_H (500 MHz, $CDCl_3$) 4.04 (s, 2H), 4.60 (dd, 2H, *J* 1.5, 4.5), 5.21 (dd, 1H, *J* 1.5, 10.0), 5.28 (dd, 1H, *J* 1.5, 17.0), 5.89 (m, 1H), 7.35 (d, 1H, *J* 7.5), 7.46 (t, 1H, *J* 7.5), 7.58 (t, 1H, *J* 7.5), 8.09 (d, 1H, *J* 7.5). δ_C (125 MHz, $CDCl_3$) 39.8, 66.0, 118.7, 125.4, 128.8, 132.0, 133.6, 133.8, 148.5, 169.8. *m/z* (ESI) 222.3 $[M+H]^+$. *m/z* (HRMS-ESI) 222.0733 $[M+H]^+$; $C_{11}H_{12}NO_4$ requires 222.0761.

*Ethyl-2-phenylacetate (**19**)*

Yield: 80 %, pale yellow oil. δ_H (500 MHz, $CDCl_3$) 1.23 (t, 3H, *J* 7.0), 3.56 (s, 2H), 4.13 (q, 2H, *J* 7.0), 7.29 (m, 5H). δ_C (125 MHz, $CDCl_3$) 14.2, 41.4, 60.8, 128.0, 134.3, 171.6. *m/z* (HRMS-ESI) 165.0914 $[M+H]^+$; $C_{10}H_{13}O_2$ requires 165.0910.

*Ethyl-2-(2-chlorophenyl)acetate (**20**)*

Yield: 71 %, pale yellow oil. δ_H (500 MHz, $CDCl_3$) 1.20 (t, 3H, *J* 7.0), 3.71 (s, 2H), 4.12 (q, 2H, *J* 7.0), 7.23 (m, 4H). δ_C (125 MHz, $CDCl_3$) 14.0, 38.9, 60.7, 128, 132.4, 134.3, 170.5. *m/z* (HRMS-ESI) 199.0526 $[M+H]^+$; $C_{10}H_{12}ClO_2$ requires 199.0520.

General Procedure for the Synthesis of N-Alkyl or N-Aryl-2-(2-nitrophenyl)acetamides **16**–**18**

A dry round-bottom flask was charged under $N_2$with 2-nitrophenylacetic acid (324 mg, 1.79 mmol), amine (2.42 mmol), *O*-(Benzotriazol-1-yl)-*N*,*N*,*N*′,*N*′-tetramethyluronium hexafluorophosphate (HBTU, 709 mg, 1.87 mmol), and CH_2Cl_2 (10 mL) before adding *N*,*N*-diisopropylethylamine (DIPEA, 3.85 mmol). The solution was stirred at room temperature while monitoring by TLC analysis (petroleum spirit/acetone, 80 : 20). On complete consumption of starting material, the reaction was diluted with CH_2Cl_2 (30 mL) and washed with 5 % HCl (3 × 25 mL), saturated aqueous Na_2CO_3 (3 × 25 mL), and brine (30 mL). The organic layer was dried over anhydrous $MgSO_4$ and concentrated to afford the pure amide.

*N-Ethyl-2-(2-nitrophenyl)acetamide (**16**)*

57 %, white amorphous solid; mp 137–139°C. δ_H (500 MHz, $CDCl_3$) 1.13 (t, 3H, *J* 7.0), 3.29 (q, 2H, *J* 7.0), 3.81 (s, 2H), 5.80 (br s, 1H), 7.45 (t, 1H, *J* 7.5), 7.50 (d, 1H, *J* 7.5), 7.60 (t, 1H, *J* 7.5), 8.02 (d, 1H, *J* 8.5). δ_C (125 MHz, $CDCl_3$) 15.0, 35.0, 41.1, 125.3, 128.6, 130.7, 133.6, 133.8, 149.1, 169.0. *m/z* (HRMS-ESI) 209.0924 $[M+H]^+$; $C_{10}H_{13}N_2O_3$ requires 209.0921.

*N-Phenyl-2-(2-nitrophenyl)acetamide (**17**)*

95 %, off-white amorphous solid; mp 141–143°C. δ_H (500 MHz, $CDCl_3$) 4.03 (s, 2H), 7.08 (t, 1H, *J* 7.5), 7.28 (t, 2H, *J* 7.5), 7.47 (m, 3H), 7.54 (d, 1H, *J* 7.0), 7.61 (t, 1H, *J* 7.5), 7.82 (br s, 1H), 8.05 (d, *J* 8.5). δ_C (125 MHz, $CDCl_3$) 41.9, 119.9, 124.4, 125.2, 128.6, 128.9, 130.0, 133.4, 133.7, 167.2. *m/z* (HRMS-ESI) 257.0929 $[M+H]^+$; $C_{14}H_{13}N_2O_3$ requires 257.0921.

*N-Benzyl-2-(2-nitrophenyl)acetamide (**18**)*

95 %, off-white amorphous solid; mp 136–138°C. δ_H (500 MHz, $CDCl_3$) 3.88 (s, 2H), 4.45 (d, 2H, *J* 6), 6.12 (br s, 1H), 7.26 (t, 3H, *J* 8.0), 7.31 (t, 2H, *J* 7.5), 7.45 (t, 1H, *J* 7.5), 7.51 (d, 1H, *J* 7.5), 7.60 (t, 1H, *J* 7.5), 8.04 (d, 1H, *J* 8.5). δ_C (125 MHz, $CDCl_3$) 40.9, 43.8, 125.1, 127.5, 127.6, 128.5, 128.7, 130.2, 133.5, 133.6, 137.9, 148.9, 169.0. *m/z* (HRMS-ESI) 271.1065 $[M+H]^+$; $C_{15}H_{15}N_2O_3$ requires 271.1077.

General Method for Condensation Reactions to Produce Alkenes (*Z*)-**3a**, (*E*)-**3b**−(*Z*)-**8a**, (*E*)-**8b**: Method a

To a dry round-bottom flask was added anhydrous potassium carbonate (1.205 g, 8.73 mmol) in dry THF (15 mL) under N_2followed by 18-crown-6 (0.575 g, 2.18 mmol). The mixture was stirred at room temperature for 10 min before adding a solution of the appropriate 2-(2-nitrophenyl)acetate or acetamide (4.36 mmol) in dry THF (10 mL) and heating at reflux for 3 h. Methyl 2-formyl-3,5-dimethyl-1*H*-pyrrole-1-carboxylate **12** (0.789 g, 4.36 mmol) was diluted in dry THF (8 mL) and added dropwise over 15 min to the stirring solution. The mixture was then heated at reflux for a further 16 h. The reaction was quenched with water (30 mL), transferred to a separating funnel, and extracted with EtOAc (3 × 40 mL). The combined organic layers were washed with saturated aqueous Na_2CO_3 (2 × 50 mL) and brine (2 × 50 mL), dried over anhydrous $MgSO_4$, and concentrated under vacuum. The crude product was purified by silica gel column chromatography using a petroleum spirit/acetone gradient of 100 : 0 to 80 : 20 to provide mixtures of the (*Z*)- and (*E*)-isomers.

*(Z)-Ethyl 3-(3,5-Dimethyl-1H-pyrrol-2-yl)-2-(2-nitrophenyl)acrylate ((Z)-**3a**)*

42 %, red crystalline solid; mp 124–126°C. R_f 0.50 (70 : 30 hexane/acetone). δ_H (500 MHz, $CDCl_3$) 1.13 (t, 3H, *J* 7.0), 2.17 (s, 3H), 2.35 (s, 3H), 4.12 (q, 2H, *J* 7.0), 5.90 (s, 1H), 6.82 (s, 1H), 7.43 (m, 1H), 7.62 (t, 2H, *J* 8.0), 8.02 (d, 1H, *J* 8.0), 11.89 (br s, 1H). δ_C (125 MHz, $CDCl_3$) 13.7, 14.1, 29.9, 62.1, 111.5, 112.7, 124.1, 124.6, 127.8, 129.9, 131.5, 132.5, 133.5, 134.3, 137.5, 148.5, 163.8. v_{max} (neat)/cm^{-1} 3275, 2354, 1684, 1577, 1569, 1544, 1518, 1367, 1335, 1319, 1262, 1196, 1153, 1026, 830, 789, 710. *m/z* (HRMS-ESI) 315.1350 $[M+H]^+$; $C_{17}H_{19}N_2O_4$ requires 315.1339.

*(E)-Ethyl 3-(3,5-Dimethyl-1H-pyrrol-2-yl)-2-(2-nitrophenyl)acrylate ((E)-**3b**)*

35 %, red crystalline solid; mp 117–119°C. R_f 0.26 (70 : 30 hexane /acetone). δ_H (500 MHz, $CDCl_3$) 1.19 (t, 3H, *J* 7.0), 1.95 (s, 3H), 2.19 (s, 3H), 4.10 (dq, 1H, *J* 4.0, 7.0), 4.23 (dq, 1H, *J* 3.7, 7.0), 5.74 (s, 1H), 6.80 (br s, 1H), 7.49 (t, 1H, *J* 7.5), 7.59 (t, 1H, *J* 7.5), 7.67 (t, 1H, *J* 7.5), 7.75 (s, 1H), 8.19 (d, 1H, *J* 7.5). δ_C (125 MHz, $CDCl_3$) 11.3, 13.2, 14.1, 60.8, 110.7, 116.6, 123.4, 125.6, 127.2, 129.2, 130.1, 132.5, 133.3, 133.4, 136.7, 149.2, 166.6. v_{max} (neat)/cm^{-1} 3447, 3421, 1700, 1618, 1607, 1564, 1518, 1338, 1180, 1147, 1093, 795. *m/z* (HRMS-ESI) 315.1337 $[M+H]^+$; $C_{17}H_{19}N_2O_4$ requires 315.1339.

*(Z)-Methyl 3-(3,5-Dimethyl-1H-pyrrol-2-yl)-2-(2-nitrophenyl)acrylate ((Z)-**4a**)*

36 %, red crystalline solid; mp 66–68°C. R_f 0.47 (80 : 20 petroleum spirit/acetone). δ_H (500 MHz, $CDCl_3$) 2.14 (s, 3H),

2.32 (s, 3H), 3.61 (s, 3H), 5.88 (s, 1H), 6.79 (s, 1H), 7.40 (d, 1H, *J* 7.5), 7.41 (t, 1H, *J* 7.5), 7.59 (t, 1H, *J* 7.5), 8.00 (d, 1H, *J* 7.5), 11.82 (br s, 1H). δ_C (125 MHz, $CDCl_3$) 11.8, 13.9, 52.0, 111.6, 114.0, 124.5, 124.6, 128.0, 131.5, 134.4, 137.3, 148.5, 168.2. ν_{max} (neat)/cm^{-1} 3455, 1691, 1603, 1555, 1522, 1430, 1343, 1222, 1190, 1172, 1149, 789, 718. *m/z* (HRMS-ESI) 301.1185 $[M+H]^+$. $C_{16}H_{17}N_2O_4$ requires 301.1183.

*(E)-Methyl 3-(3,5-Dimethyl-1H-pyrrol-2-yl)-2-(2-nitrophenyl)acrylate ((E)-**4b**)*

40 %, red crystalline solid; mp 90–93°C. R_f 0.36 (80 : 20 petroleum spirit/acetone). δ_H (500 MHz, $CDCl_3$) 1.95 (s, 3H), 2.20 (s, 3H), 3.70 (s, 3H), 5.74 (s, 1H), 6.74 (br s, 1H), 7.50 (d, 1H, *J* 7.5), 7.61 (t, 1H, *J* 7.5), 7.68 (t, 1H, *J* 7.5), 7.75 (s, 1H), 8.20 (d, 1H, *J* 7.5). δ_C (126 MHz, $CDCl_3$) 11.6, 13.4, 52.3, 111.0, 116.3, 123.6, 125.5, 127.6, 129.4, 130.6, 132.7, 133.4, 133.8, 134.1, 149.4, 167.4. ν_{max} (neat)/cm^{-1} 3293, 1689, 1570, 1544, 1518, 1432, 1365, 1334, 1317, 1263, 1195, 1180, 1151, 788, 709. *m/z* (HRMS-ESI) 301.1182 $[M+H]^+$; $C_{16}H_{17}N_2O_4$ requires 301.1183.

*(Z)-Allyl 3-(3,5-Dimethyl-1H-pyrrol-2-yl)-2-(2-nitrophenyl)acrylate ((Z)-**5a**)*

41 %, deep-red crystalline solid; mp 70–72°C. R_f 0.50 (80 : 20 petroleum spirit/acetone). δ_H (500 MHz, $CDCl_3$) 2.17 (s, 3H), 2.35 (s, 3H), 4.56 (d, 2H, *J* 5.5), 5.10 (dd, 1H, *J* 1.5, 13.0), 5.13 (dd, 1H, *J* 1.5, 6.5), 5.79 (m, 1H), 5.90 (s, 1H), 6.82 (s, 1H), 7.43 (d, 1H, *J* 7.5), 7.44 (t, 1H, *J* 7.5), 7.62 (t, 1H, *J* 7.5), 8.04 (d, 1H, *J* 7.5), 12.91 (br s, 1H). δ_C (125 MHz, $CDCl_3$) 11.7, 13.8, 65.7, 111.6, 114.2, 118.1, 124.6, 124.7, 127.9, 131.5, 131.6, 132.9, 133.5, 134.4, 137.4, 148.9, 167.3. ν_{max} (neat)/cm^{-1} 3300, 2360, 1685, 1577, 1570, 1542, 1517, 1507, 1364, 1312, 1182, 1144, 966, 932, 858, 790. *m/z* (HRMS-ESI) 327.1342 $[M+H]^+$; $C_{18}H_{19}N_2O_4$ requires 327.1339.

*(E)-Allyl 3-(3,5-Dimethyl-1H-pyrrol-2-yl)-2-(2-nitrophenyl)acrylate ((E)-**5b**)*

33 %, red crystalline solid; mp 102–105°C. R_f 0.40 (80 : 20 petroleum spirit/acetone). δ_H (500 MHz, $CDCl_3$) 1.95 (s, 3H), 2.19 (s, 3H), 4.59 (dd, 1H, *J* 5.5, 13.5), 4.64 (dd, 1H, *J* 5.5, 13.5), 5.15 (dd, 1H, *J* 1.5, 10.0), 5.18 (dd, 1H, *J* 1.5, 18.5), 5.74 (s, 1H), 5.85 (m, 1H), 6.75 (br s, 1H), 7.50 (d, 1H, *J* 8.0), 7.60 (t, 1H, *J* 8.0), 7.68 (t, 1H, *J* 8.0), 7.77 (s, 1H), 8.19 (d, 1H, *J* 8.0). δ_C (125 MHz, $CDCl_3$) 11.5, 13.4, 65.6, 111.0, 116.3, 117.7, 123.6, 125.4, 127.6, 129.5, 130.6, 132.5, 133.3, 133.7, 134.1, 149.4, 166.5. ν_{max} (neat)/cm^{-1} 3455, 1687, 1610, 1557, 1524, 1343, 1257, 1232, 1068, 869, 733. *m/z* (HRMS-ESI) 327.1333 $[M+H]^+$; $C_{17}H_{19}N_2O_4$ requires 327.1339.

*(Z)-3-(3,5-Dimethyl-1H-pyrrol-2-yl)-N-ethyl-2-(2-nitrophenyl)acrylamide ((Z)-**6a**)*

21 %, red crystalline solid; mp 96–99°C. R_f 0.17 (80 : 20 petroleum spirit/acetone). δ_H (500 MHz, $CDCl_3$) 1.07 (t, 3H, *J* 7.0), 2.09 (s, 3H), 2.31 (s, 3H), 3.31 (q, 2H, *J* 7.0), 5.18 (br s, 1H), 5.82 (s, 1H), 6.46 (s, 1H), 7.52 (m, 2H), 7.65 (t, 1H, *J* 8.0), 7.98 (d, 1H, *J* 8.0), 12.21 (br s, 1H). δ_C (125 MHz, $CDCl_3$) 11.3, 13.5, 14.6, 34.8, 110.6, 116.4, 124.0, 124.7, 128.0, 128.7, 128.8, 132.9, 133.3, 133.4, 136.3, 149.5, 167.5. ν_{max} (neat)/cm^{-1} 3408, 1639, 1576, 1569, 1517, 1457, 1350, 1224. *m/z* (HRMS-ESI) 314.1497 $[M+H]^+$; $C_{17}H_{20}N_3O_3$ requires 314.1499.

*(Z)-3-(3,5-Dimethyl-1H-pyrrol-2-yl)-2-(2-nitrophenyl)-N-phenylacrylamide ((Z)-**7a**)*

22 %, red crystalline solid; mp 177–179°C. R_f 0.36 (80 : 20 petroleum spirit/acetone). δ_H (500 MHz, $CDCl_3$) 2.12 (s, 3H), 2.32 (s, 3H), 5.86 (s, 1H), 6.56 (s, 1H), 6.87 (br s, 1H), 7.12 (t, 1H, *J* 7.5), 7.32 (t, 2H, *J* 7.5), 7.37 (t, 2H, *J* 7.5), 7.56 (t, 1H, *J* 8.0), 7.60 (d, 1H, *J* 8.0), 7.71 (t, 1H, *J* 8.0), 8.03 (d, 1H, *J* 8.0), 12.00 (br s, 1H). δ_C (125 MHz, $CDCl_3$) 11.4, 13.6, 111.1, 115.6, 121.4, 124.1, 124.9, 129.0, 129.1, 130.1, 133.5, 133.5, 133.8, 135.8, 137.4, 149.7, 166.2. ν_{max} (neat)/cm^{-1} 3400, 1650, 1595, 1592, 1518, 1498, 1436, 1362, 1352, 1318, 1229, 1188, 1151, 1004, 802, 790, 772, 759, 739, 718. *m/z* (HRMS-ESI) 362.1521 $[M+H]^+$; $C_{21}H_{20}N_3O_3$ requires 362.1499.

*(E)-3-(3,5-Dimethyl-1H-pyrrol-2-yl)-2-(2-nitrophenyl)-N-phenylacrylamide ((E)-**7b**)*

<5 %, red amorphous solid (impure, not tested in angiogenesis inhibition assay). δ_H (500 MHz, $CDCl_3$) 1.92 (s, 3H), 2.13 (s, 3H), 5.70 (s, 1H), 6.47 (br s, 1H), 7.04 (t, 1H, *J* 7), 7.14 (br s, 1H), 7.24 (t, 2H, *J* 7.5), 7.43 (d, 2H, *J* 8.0), 7.57 (d, 1H, *J* 7.5), 7.68 (s, 1H), 7.75 (t, 1H, *J* 7.5), 7.66 (m, 1H), 8.13 (d, 1H, *J* 8.0). δ_C (125 MHz, $CDCl_3$) 11.2, 13.1, 110.6, 118.9, 120.4, 123.3, 124.1, 125.1, 125.4, 128.7, 129.6, 130.3, 131.5, 133.5, 133.8, 134.3, 138.0, 149.4, 165.0. *m/z* (HRMS-ESI) 362.1503 $[M+H]^+$; $C_{21}H_{20}N_3O_3$ requires 362.1499.

*(Z)-N-Benzyl-3-(3,5-dimethyl-1H-pyrrol-2-yl)-2-(2-nitrophenyl)acrylamide ((Z)-**8a**)*

16 %, red crystalline solid; mp 140–142°C. R_f 0.36 (80 : 20 petroleum spirit/acetone). δ_H (500 MHz, $CDCl_3$) 2.09 (s, 3H), 2.31 (s, 3H), 4.50 (d, 2H, *J* 6), 5.50 (br s, 1H), 5.83 (s, 1H), 6.48 (s, 1H), 7.20 (d, 2H, *J* 8.0), 7.22 (m, 1H, *J* 7.0), 7.28 (t, 2H, *J* 7.5), 7.47 (m, 1H, *J* 8.0), 7.49 (m, 1H, *J* 6.5), 7.61 (t, 1H, *J* 7.5), 7.94 (d, 1H, *J* 8.5), 12.21 (br s, 1H). δ_C (125 MHz, $CDCl_3$) 11.3, 13.7, 43.9, 110.7, 115.8, 124.0, 124.7, 127.3, 127.3, 128.3, 128.6, 128.9, 129.2, 133.1, 133.3, 133.4, 136.0, 138.0, 167.6. ν_{max} (neat)/cm^{-1} 3435, 1643, 1570, 1543, 1507, 1453, 1362, 1341, 1316, 1237, 1217, 1150, 786, 728, 709. *m/z* (HRMS-ESI) 376.1668 $[M+H]^+$; $C_{22}H_{22}N_3O_3$ requires 376.1656.

*(E)-N-Benzyl-3-(3,5-dimethyl-1H-pyrrol-2-yl)-2-(2-nitrophenyl)acrylamide ((E)-**8b**)*

<5 %, red amorphous solid (impure, not tested in angiogenesis inhibition assay). δ_H (500 MHz, $CDCl_3$) 2.09 (s, 3H), 2.31 (s, 3H), 4.50 (d, 2H, *J* 6), 5.50 (br s, 1H), 5.83 (s, 1H), 6.48 (s, 1H), 7.20 (d, 2H, *J* 8.0), 7.22 (m, 1H, *J* 7.0), 7.28 (t, 2H, *J* 7.5), 7.47 (m, 1H, *J* 8.0), 7.49 (m, 1H, *J* 6.5), 7.61 (t, 1H, *J* 7.5), 7.94 (d, 1H, *J* 8.5). Note: owing to impurities, the chemical shift of the pyrrolic NH signal could not be assigned unambiguously. δ_C (125 MHz, $CDCl_3$) 11.3, 13.6, 43.9, 110.7, 115.8, 124.0, 124.7, 127.3, 127.3, 128.4, 128.6, 128.9, 129.3, 133.088, 133.3, 133.4, 136.0, 137.974, 167.6. *m/z* (HRMS-ESI) 376.1675 $[M+H]^+$; $C_{22}H_{22}N_3O_3$ requires 376.1656.

General Method for Condensation Reactions to Produce Alkenes (Z)-**9a**, (E)-**9b** and (Z)-**10a**, (E)-**10b**: Method b

Dry *N*,*N*-diisopropylamine (4.60 mmol) was dissolved in dry THF (7 mL) under Ar in a three-neck 100-mL round-bottom flask. The flask was cooled to −78°C and *n*-butyllithium (4.60 mmol) was added and stirred for 20 min. Ethyl-2-phenylacetate **19** or ethyl-2-(2-chlorophenyl)acetate **20** (4.28 mmol)

was then added dropwise as a solution in dry THF (1 mL) and the reaction mixture was stirred for a further 30 min. Methyl 2-formyl-3,5-dimethyl-1*H*-pyrrole-1-carboxylate **12** (0.757 g, 4.18 mmol) was subsequently added dropwise as a solution in dry THF (1 mL) and the reaction stirred for a further 30 min, with monitoring by TLC (75 : 25 petroleum spirit/EtOAc). The reaction was quenched with saturated aqueous NH_4Cl (30 mL) and the solvent removed under vacuum. EtOAc (30 mL) was added to the residue and the organic layer was washed with saturated aqueous NH_4Cl (3×25 mL), saturated aqueous Na_2CO_3 (2×25 mL), and brine (30 mL), before being dried over anhydrous $MgSO_4$ and concentrated under vacuum. The crude product was purified by silica gel chromatography column with a gradient from 100 : 0 to 70 : 30 petroleum spirit/EtOAc to provide mixtures of the (*Z*)- and (*E*)-isomers.

(E)-Ethyl 3-(3,5-Dimethyl-1H-pyrrol-2-yl)-2-phenylacrylate ((E)-**9b**)

32 %, yellow crystalline solid; mp 62–64°C. R_f 0.43 (75 : 25 petroleum spirit/EtOAc). δ_H (500 MHz, $CDCl_3$) 1.26 (t, 3H, *J* 7.0), 1.91 (s, 3H), 2.19 (s, 3H), 4.22 (q, 2H, *J* 7.0), 5.69 (s, 1H), 6.84 (br s, 1H), 7.32 (d, 2H, *J* 7.0), 7.43 (t, 1H, *J* 7.0), 7.46 (t, 2H, *J* 7.0), 7.75 (s, 1H). δ_C (125 MHz, $CDCl_3$) 11.2, 13.1, 14.4, 60.5, 110.0, 120.5, 124.1, 127.4, 127.9, 128.8, 129.0, 130.2, 132.9, 137.3, 169.2. ν_{max} (neat)/cm^{-1} 3442, 1697, 1607, 1560, 1497, 1227. *m/z* (HRMS-ESI) 270.1488 $[M+H]^+$; $C_{17}H_{20}NO_2$ requires 270.1489.

(Z)-Ethyl 3-(3,5-Dimethyl-1H-pyrrol-2-yl)-2-(2-chlorophenyl)acrylate ((Z)-**10a**)

5 %, yellow crystalline solid; mp 124–126°C. R_f 0.71 (70 : 30 petroleum spirit/EtOAc). δ_H (500 MHz, $CDCl_3$) 1.20 (t, 3H, *J* 7.0), 2.14 (s, 3H) 2.33 (s, 3H), 4.20 (q, 2H, *J* 7.0), 5.87 (s, 1H), 6.72 (s, 1H), 7.25 (m, 2H), 7.31 (d, 1H, *J* 7.0), 7.38 (d, 1H, *J* 7.0), 11.80 (br s, 1H). δ_C (125 MHz, $CDCl_3$) 11.6, 13.8, 14.3, 61.0, 111.3, 116.1, 124.4, 126.9, 128.3, 129.2, 130.6, 131.8, 132.2, 133.6, 135.1, 141.2, 168.9. ν_{max} (neat)/cm^{-1} 3273, 1680, 1576, 1545, 1465, 1188, 736. *m/z* (HRMS-ESI) 304.1099 $[M+H]^+$; $C_{17}H_{19}NO_2Cl$ requires 304.1099.

(E)-Ethyl 3-(3,5-Dimethyl-1H-pyrrol-2-yl)-2-(2-chlorophenyl)acrylate ((E)-**10b**)

41 %, yellow amorphous solid; mp 70–74°C. R_f 0.39 (75 : 25 petroleum spirit/EtOAc). δ_H ($CDCl_3$, 500 MHz) 1.24 (t, 3H, *J* 7.0), 1.93 (s, 3H), 2.20 (s, 3H), 4.18 (q, 1H, *J* 7.0), 4.25 (q, 2H, *J* 7.0), 5.74 (s, 1H,), 6.75 (br s, 1H), 7.3 (m, 3H), 7.54 (d, 1H, *J* 8), 7.78 (s, 1H). δ_C (125 MHz, $CDCl_3$) 11.2, 13.1, 14.3, 60.6, 110.3, 117.7, 123.9, 127.3, 128.1, 129.5, 129.5, 130.1, 131.9, 133.5, 135.1, 136.3, 167.4. ν_{max} (neat)/cm^{-1} 3447, 1697, 1603, 1558, 1473, 1226, 745. *m/z* (HRMS-ESI) 304.1092 $[M+H]^+$; $C_{17}H_{19}NO_2Cl$ requires 304.1099.

X-Ray Crystallography

Crystal Data

Compound (*Z*)-**5a**. $C_{18}H_{18}N_2O_4$, $M = 326.35$, $T = 200$ K; monoclinic, space group $P2_1/c$, $Z = 4$; $a = 12.5669(4)$ Å, $b = 7.9086(3)$ Å, $c = 17.6200(4)$ Å; $\beta = 103.730(2)°$ $V = 1701.15(6)$ Å^3; $D_x = 1.274$ g cm^{-3}; 32664 reflections measured ($2\theta = 5$–$55°$) merged to 3903 unique data; $R = 0.053$ (for 2656 data with $I > 2\sigma(I)$), $R_w = 0.147$ (all data); $S = 0.95$.

Compound (*E*)-**5b**. $C_{18}H_{18}N_2O_4$, $M = 326.35$, $T = 298(2)$ K; triclinic, space group *P*-1, $Z = 2$; $a = 8.4326(4)$ Å, $b = 10.2147(4)$ Å, $c = 11.0598(6)$ Å; $\alpha = 72.485(3)°$, $\beta = 76.605(2)°$, $\gamma = 71.312(3)°$; $V = 850.89(7)$ Å^3; $D_x = 1.274$ g cm^{-3}; 7615 reflections measured ($2\theta = 4$–$54.2°$) merged to 3674 unique data $R = 0.064$ (for 2849 data with $I > 2\sigma(I)$), $R_w = 0.187$ (all data); $S = 0.99$.

Structure Determination

Images were measured on Nonius Kappa CCD diffractometers (Mo $K\alpha$ radiation, graphite monochromator, λ 0.71073 Å) and data were extracted using the *DENZO* package.[26] For (*Z*)-**5a**, structure solution was by direct methods (*SIR92*)[27] and the structure was refined using the *CRYSTALS* program package.[28] For (*E*)-**5b**, structure solution was by direct methods (*SIR97*)[29] and the structure was refined using the *SHELXL-97* program package.[30] Atomic coordinates, bond lengths and angles, and displacement parameters have been deposited at the Cambridge Crystallographic Data Centre (CCDC accession numbers 905343 and 905344 respectively). These data can be obtained free of charge via www.ccdc.cam.ac.uk/data_requerst/cif, by emailing data_request@ccdc.cam.ac.uk, or by contacting The Cambridge Crystallographic Data Centre, 12 Union Road, Cambridge CB2 1EZ, UK; fax: +44 1223 336033.

Angiogenesis Inhibition Assay

Compounds were tested for angiogenesis inhibition in 48-well culture plates using the previously reported in vitro assay with some modifications.[23] Briefly, the thoracic aortas from female Fischer 344 rats were excised and the 2.5-cm-long vessels placed in Hank's buffered salt solution (HBSS) media containing 2.5 μg mL^{-1} amphotericin B and cross-sectioned at 1-mm intervals. In the angiogenesis assay, 15 μL of bovine thrombin (50 NIH unit mL^{-1} in 0.15 M NaCl) was added to each well, followed by 0.5 mL per well of 3 mg mL^{-1} bovine fibrinogen in Medium 199. The thrombin and fibrinogen were mixed rapidly and one vessel section was quickly placed in the centre of the well before clot formation. Fibrin gel formation usually occurred within 0.5 min, leaving the vessel fragment suspended in the gel. On gel formation, 0.5 mL per well of Medium 199 supplemented with 20 % foetal calf serum (FCS), 0.1 % 6-aminohexanoic acid, L-glutamine, and antibiotics (gentamicin sulfate and amphotericin B), and test compound were added. Six replicate cultures were examined for each concentration of test compound. Vessels were cultured at 37°C in 5 % CO_2 in a humidified environment for 7 days, with the medium being changed on Day 4. On Day 5, the percentage of the field of view occupied by vessel outgrowths (FOV occupancy %) was used as a quantitative measure of angiogenesis (inhibition) relative to control (no compound added).

Supplementary Material

Supplementary material consisting of ^{1}H NMR spectra for (*Z*)-**3a** and (*E*)-**3b** and angiogenesis inhibition assay statistics is available on the Journal's website.

Acknowledgements

P. Sudta and S. Suksamrarn acknowledge financial support from the Thailand Research Fund through the Royal Golden Jubilee PhD Program. S. Prapbai and P. Kongsaeree thank the National Research University Project through Mahidol University for financial support. M. Kelso acknowledges partial financial support from the University of Wollongong University Research Council (URC) Small Grants Scheme. A. Bezos and C. R. Parish acknowledge support from an Australian National Health and Medical Research Council (NHMRC) Program Grant.

References

[1] D. Hanahan, J. Folkman, *Cell* **1996**, *86*, 353. doi:10.1016/S0092-8674(00)80108-7

[2] P. Carmeliet, *Nat. Med.* **2003**, *9*, 653. doi:10.1038/NM0603-653

[3] B. R. Zetter, *Annu. Rev. Med.* **1998**, *49*, 407. doi:10.1146/ANNUREV.MED.49.1.407

[4] F. Shojaei, *Cancer Lett.* **2012**, *320*, 130. doi:10.1016/J.CANLET.2012.03.008

[5] H. Hurwitz, L. Fehrenbacher, W. Novotny, T. Cartwright, J. Hainsworth, W. Heim, J. Berlin, A. Baron, S. Griffing, E. Holmgren, N. Ferrara, G. Fyfe, B. Rogers, R. Ross, F. Kabbinavar, *N. Engl. J. Med.* **2004**, *350*, 2335. doi:10.1056/NEJMOA032691

[6] A. Sandler, R. Gray, M. C. Perry, J. Brahmer, J. H. Schiller, A. Dowlati, R. Lilenbaum, D. H. Johnson, *N. Engl. J. Med.* **2006**, *355*, 2542. doi:10.1056/NEJMOA061884

[7] K. Miller, M. Wang, J. Gralow, M. Dickler, M. Cobleigh, E. A. Perez, T. Shenkier, D. Cella, N. E. Davidson, *N. Engl. J. Med.* **2007**, *357*, 2666. doi:10.1056/NEJMOA072113

[8] J. Holash, S. Davis, N. Papadopoulos, S. D. Croll, L. Ho, M. Russell, P. Boland, R. Leidich, D. Hylton, E. Burova, E. Ioffe, T. Huang, C. Radziejewski, K. Bailey, J. P. Fandl, T. Daly, S. J. Wiegand, G. D. Yancopoulos, J. S. Rudge, *Proc. Natl. Acad. Sci. USA* **2002**, *99*, 11393. doi:10.1073/PNAS.172398299

[9] A.-M. O'Farrell, T. J. Abrams, H. A. Yuen, T. J. Ngai, S. G. Louie, K. W. H. Yee, L. M. Wong, W. Hong, L. B. Lee, A. Town, B. D. Smolich, W. C. Manning, L. J. Murray, M. C. Heinrich, J. M. Cherrington, *Blood* **2003**, *101*, 3597. doi:10.1182/BLOOD-2002-07-2307

[10] W. T. A. van der Graaf, J.-Y. Blay, S. P. Chawla, D.-W. Kim, B. Bui-Nguyen, P. G. Casali, P. Schöffski, M. Aglietta, A. P. Staddon, Y. Beppu, A. Le Cesne, H. Gelderblom, I. R. Judson, N. Araki, M. Ouali, S. Marreaud, R. Hodge, M. R. Dewji, C. Coens, G. D. Demetri, C. D. Fletcher, A. P. Dei Tos, P. Hohenberger, *Lancet* **2012**, *379*, 1879. doi:10.1016/S0140-6736(12)60651-5

[11] P. Kupsch, B. F. Henning, K. Passarge, H. Richly, K. Wiesemann, R. A. Hilger, M. E. Scheulen, O. Christensen, E. Brendel, B. Schwartz, E. Hofstra, R. Voigtmann, S. Seeber, D. Strumberg, *Clin. Colorectal Cancer* **2005**, *5*, 188. doi:10.3816/CCC.2005.N.030

[12] X. Wu, Y. Jin, I. H. Cui, Z. Xu, Y. Zhang, X. Zhang, C. Tang, Y. Gong, J. Chen, *Anticancer Drugs* **2012**, *23*, 731. doi:10.1097/CAD.0B013E32835514F4

[13] L. Wood, *Expert Opin. Pharmacother.* **2012**, *13*, 1323. doi:10.1517/14656566.2012.689130

[14] V. P. Koshenkov, S. E. Rodgers, *Curr. Opin. Oncol.* **2012**, *24*, 414. doi:10.1097/CCO.0B013E328353D774

[15] C. Zhou, J. Zhang, Y. Zheng, Z. Zhu, *Int. J. Cancer* **2012**, *131*, 1013. doi:10.1002/IJC.27543

[16] R. Roskoski, Jr, *Biochem. Biophys. Res. Commun.* **2007**, *356*, 323. doi:10.1016/J.BBRC.2007.02.156

[17] C. R. Prakash, S. Raja, *Mini Rev. Med. Chem.* **2012**, *12*, 98. doi:10.2174/138955712798995039

[18] L. Sun, C. Liang, S. Shirazian, Y. Zhou, T. Miller, J. Cui, J. Y. Fukuda, J.-Y. Chu, A. Nematalla, X. Wang, H. Chen, A. Sistla, T. C. Luu, F. Tang, J. Wei, C. Tang, *J. Med. Chem.* **2003**, *46*, 1116. doi:10.1021/JM0204183

[19] A. D. Abell, B. K. Nabbs, A. R. Battersby, *J. Am. Chem. Soc.* **1998**, *120*, 1741. doi:10.1021/JA973656+

[20] J.-R. Schauder, S. Jendrezejewski, A. Abell, G. J. Hart, A. R. Battersby, *J. Chem. Soc. Chem. Commun.* **1987**, 436. doi:10.1039/C39870000436

[21] E. Arunan, G. R. Desiraju, R. A. Klein, J. Sadlej, S. Scheiner, I. Alkorta, D. C. Clary, R. H. Crabtree, J. J. Dannenberg, P. Hobza, H. G. Kjaergaard, A. C. Legon, B. Mennucci, D. J. Nesbitt, *Pure Appl. Chem.* **2011**, *83*, 1637. doi:10.1351/PAC-REC-10-01-02

[22] L. Sun, N. Tran, F. Tang, H. App, P. Hirth, G. McMahon, C. Tang, *J. Med. Chem.* **1998**, *41*, 2588. doi:10.1021/JM980123I

[23] K. J. Brown, S. F. Maynes, A. Bezos, D. J. Maguire, M. D. Ford, C. R. Parish, *Lab. Invest.* **1996**, *75*, 539.

[24] C. R. Parish, C. Freeman, K. J. Brown, D. J. Francis, W. B. Cowden, *Cancer Res.* **1999**, *59*, 3433.

[25] P.-J. Chen, S. Chang, Medigen Biotechnology Corporation, A Phase III Study of PI-88 in the Adjuvant Treatment of Subjects with Hepatitis Virus Related Hepatocellular Carcinoma After Surgical Resection. Available at http://www.cancer.gov/clinicaltrials/search/view?cdrid=706994&version=HealthProfessional&protocolsearchid=11780342 (accessed 5 June 2013).

[26] Z. Otwinowski, W. Minor, in *Methods in Enzymology:Macromolecular Crystallography, Part A* (Eds C. W. Carter Jr, R. M. Sweet) 1997, Vol. 276, pp. 307–326 (Academic: New York, NY).

[27] A. Altomare, G. Cascarano, C. Giacovazzo, A. Guagliardi, M. C. Burla, G. Polidori, M. Camalli, *J. Appl. Cryst.* **1994**, *27*, 435.

[28] P. W. Betteridge, J. R. Carruthers, R. I. Cooper, K. Prout, D. J. Watkin, *J. Appl. Cryst.* **2003**, *36*, 1487. doi:10.1107/S0021889803021800

[29] A. Altomare, M. C. Burla, M. Camalli, G. L. Cascarano, C. Giacovazzo, A. Guagliardi, A. G. G. Moliterni, G. Polidori, R. Spagna, *J. Appl. Cryst.* **1999**, *32*, 115. doi:10.1107/S0021889898007717

[30] G. M. Sheldrick, *Acta Crystallogr. A* **2008**, *64*, 112. doi:10.1107/S0108767307043930